

Numerical estimation of soil compaction due to pile driving

Wolfgang Fellin*, Gernot Hochenwarter*

Summary

During pile driving soil is radially displaced. One can expect that the soil around the pile should therefore be compacted. Extensive numerical studies with several cohesionless soil models, pile diameters and initial densities showed that there is a compaction but especially for medium or high initial density or in less compactable soil there is also a loosening of the surrounding soil. The aim of this paper is to give a rough approximation of the relative density around a driven pile.

1. Numerical analysis

A finite element analysis of static pile driving up to 25 m with various soils, pile diameters and initial densities has been carried out by HOCHENWARTER [2000].

1.1. Finite element model

The subsoil was modeled by an axial-symmetric finite element mesh (Fig. 1), using axisymmetric 4-noded bilinear solid elements. The investigated soil region has a diameter of 20 m and a height of 38 m. The vertical boundaries are fixed in horizontal direction, the bottom is fixed in vertical direction, the top is free (Fig. 2). The behaviour of the soil is described by the hypoplastic constitutive law in the version of VON WOLFFERSDORFF [1996] with the parameters presented by HERLE [2000]. The hypoplastic law simulates very well the volumetric behaviour of the soil, namely the contractancy and the dilatancy.

The calculation was performed with the finite element program ABAQUS [1998]. Geometric nonlinearity (finite strain) has been taken into account. The hypoplastic constitutive law was implemented by an user defined subroutine [RODDEMAN, 1997]. ABAQUS uses the Newton-Raphson method to obtain solutions for such nonlinear problems.

The penetration of the pile was simulated by displacing the boundaries of an initial cylindrical cavity (Fig. 2). Starting with an inner boundary at the axis of symmetry ($r_0 = 0$) would give infinite strains⁽¹⁾. The influence of on the compaction was studied. It has been obtained that $r_0 = 1$ cm is a limit radius. For $r_0 < 1$ cm the calculated density doesn't change significantly. The depth of the conical pile

tip was chosen as $h = 2R$. Analysis with a more flat tip $h = R$ showed solely a slightly better compaction.

Friction between pile and soil was neglected in this simplified analysis.

1.2 Preliminary Investigations

HERLE [2000] presented hypoplastic parameters for 10 different soils. To reduce the number

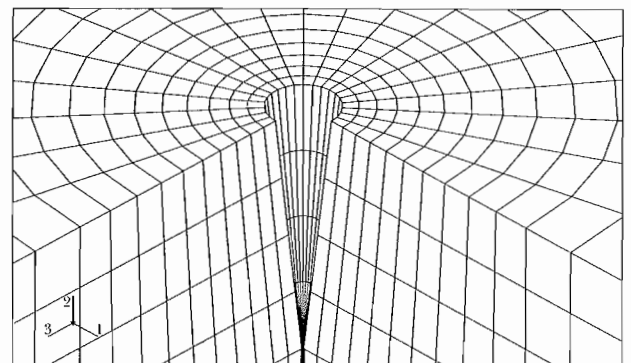


Fig. 1 – Finite element mesh.

Fig. 1 – Maglia ad elementi finiti.

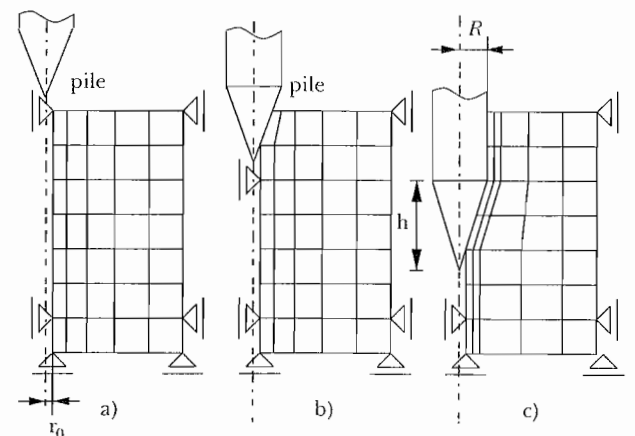


Fig. 2 – Simulation of pile driving.

Fig. 2 – Simulazione dell'infissione.

* Inst. for Geotechnics and Tunnelling, University of Innsbruck, Austria.

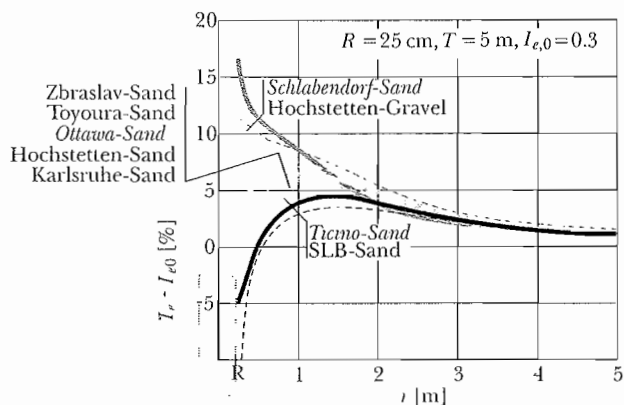


Fig. 3 - Change of relative density after pile driving up to 25 m depth. The pile has a radius of $R = 25$ cm. The relative density I_e minus the initial relative density $I_{e,0}$ is plotted in a depth of $T = 5$ m via the distance to the pile axis r . The three chosen representative soils are indicated by thick lines and bold face.

Fig. 3 - Cambiamento di densità relativa dopo infissione a 25 m di profondità. Il palo ha un raggio $R = 25$ cm. La differenza tra la densità relativa dopo l'infissione e quella iniziale è diagrammata in funzione della distanza dall'asse del palo r ad una profondità $T = 5$ m. La risposta dei tre terreni scelti come rappresentativi è indicata con curve a tratto pieno e didascalie in neretto.

of calculations three representative sands are chosen. In Fig. 3 the change of relative density $I_e = (\max e - e) / (\max e - \min e)$ compared to the initial relative density is plotted for all investigated soils. The initial relative density is $I_e = 0.3$ the pile radius is $R = 0.25$ m, the horizontal cross section is in 5 m depth. Similar results were obtained for the depths of 10, 15 and 20 m as well as in a second study with a pile radius of $R = 0.1$ m. Experimental results of DAVIDSON *et al.* [1981] for cone penetration tests show the same trends for the obtained density distribution. Similar numerical results for a particular sand are presented by CUDMANI [2000].

The soils are subdivided into three groups: well, medium and poorly compactable soils. These three groups are represented by Schlabendorf sand, Ottawa sand and Ticino sand, respectively (Fig. 3). The soils used in this finite element calculation can be classified by the help of the uniformity coefficient U , which is for well compactable soils $U \geq 3$, for medium compactable soils $1.4 < U < 2.6$ and for poorly compactable soils $U \leq 1.4$.

The compaction effect was studied in different horizontal cross sections. It has been obtained that the radial density distribution at a particular depth is no more influenced by pile driving as soon as the pile tip is 5 m deeper. This distance between tip and cross section is introduced as limit depth $T_0 = 5$ m. All presented compaction results refer to cross sections which are at least 5 m above the pile tip.

1.3. Refined Investigations

The finite element calculations were performed for all combinations of the parameters listed in Tab. I.

Tab. I - Parameters for calculation: $I_{e,0}$ initial relative density, R radius of the pile, T depth of the considered horizontal cross section; penetration depth of the pile is 25 m. Tab. I - Parametri di calcolo: $I_{e,0}$ densità relativa iniziale, R raggio del palo, T profondità della sezione orizzontale; la profondità del palo è di 25 m.

Soil	$I_{e,0}$ [-]	R [m]	T [m]
Schlabendorf sand	0.3	0.10	5
Ottawa sand	0.5	0.15	10
Ticino sand	0.8	0.20	15
		0.25	20

2. Distribution of density

The density distribution around a pile is of the typical form shown in Fig. 4. This curve can be approximately drawn when the relative density at the pile surface $I_e(R)$, the maximum relative density $\max I_e$, the location of this maximum $r(\max I_e)$ and

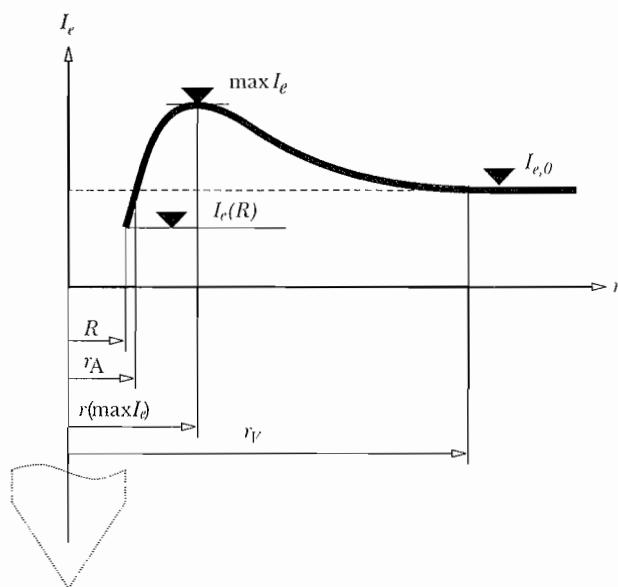


Fig. 4 - Typical compaction around a pile with radius R . The relative density I_e can be less the the initial relative density $I_{e,0}$ in a range of loosening r_A . The maximum relative density is reached at $r(\max I_e)$. Outside of r_V no compaction takes place.

Fig. 4 - Tipico andamento della compattazione attorno ad un palo di raggio R . La densità relativa dopo l'infissione I_e può essere minore di quella iniziale $I_{e,0}$ in una zona di dilatazione di raggio r_A . La massima densità relativa è raggiunta ad una distanza $r(\max I_e)$. Al di là di una distanza r_V non si ha alcuna compattazione

the range of compaction r_C are known. If there is a decrease of the density near the pile the range of loosening r_A is also given.

To estimate the characteristic points of the compaction curve the following dimensionless quantities are used:

$$I_e = \frac{\max e - e}{\max e - \min e} \dots \text{relative density}$$

$$I_{e,0} = \frac{\max e - e}{\max e - \min e} \dots \text{initial relative density}$$

$$\frac{R}{T_0} \dots \text{pile radius } T, \text{ limit radius } r_0 = 0,01 \text{ m}$$

$$\frac{T}{T_0} \dots \text{dept } T, \text{ limit } T_0 = 5 \text{ m}$$

The following equations were found by a linear least square fitting of the finite element analysis results.

2.1. Relative density at pile surface

The relative density at the pile $I_e(R)$ can be estimated by

$$I_e(R) - I_{e,0} \approx a_0 + a_1 \frac{R}{r_0} + a_2 \frac{T}{T_0} + a_3 I_{e,0} \quad (1)$$

with

compactability	a_0	a_1	a_2	a_3
well	0.30	0.00411	0.025	-0.89
medium	0.18	0.00065	0.021	-0.74
poorly	0.12	0.00275	0.020	-0.89

Curves obtained with Eq. 1 are shown in Fig. 5.

2.2. Maximum relative density

The maximum relative density can be estimated by

$$\max(I_e - I_{e,0}) \approx b_0 + b_1 \frac{R}{r_0} + b_2 \frac{T}{T_0} + b_3 I_{e,0} + b_4 I_{e,0}^2 \quad (2)$$

with

compactability	b_0	b_1	b_2	b_3	b_4
well	0.391	0.00230	0.011	-1.22	0.859
medium	0.079	0.00073	0.006	-0.14	0.057
poorly	0.068	0.00003	0.004	-0.09	0.032

Curves obtained with Eq. 2 are shown in Fig. 6.

The location of the maximum density can be estimated by

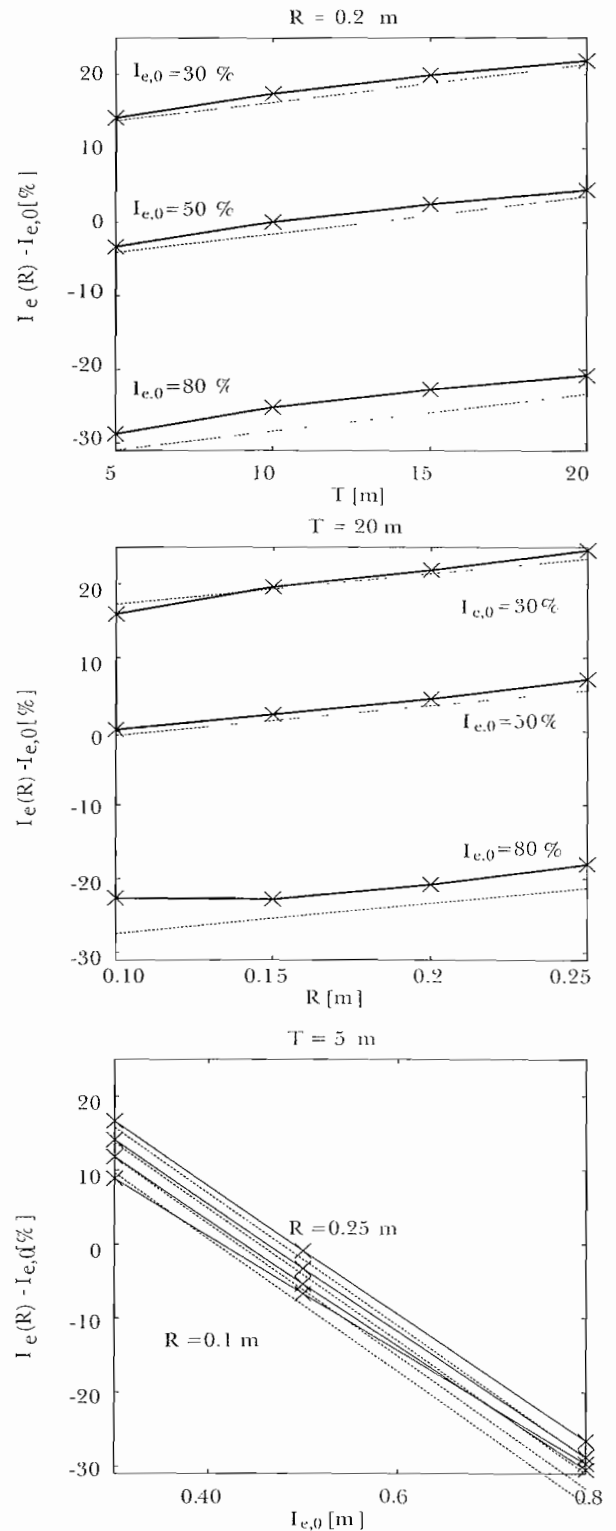


Fig. 5 - Relative density at the pile $I_e(R)$ minus initial relative density $I_{e,0}$ for well compactable soil (Schlabendorf sand) after pile driving. Continuous lines are results of finite element analysis; dash-dotted lines are results of Eq. 1. R is the pile radius, T is the depth.

Fig. 5 - Differenza tra densità relativa finale ed iniziale all'interfaccia con il palo, $I_e(R)$, per un terreno ben compattabile (sabbia di schlabendorf). Le linee continue sono i risultati delle analisi ad elementi finiti; le linee tratteggiate sono i risultati dell'equazione 1. R è il raggio del palo e T è la profondità.

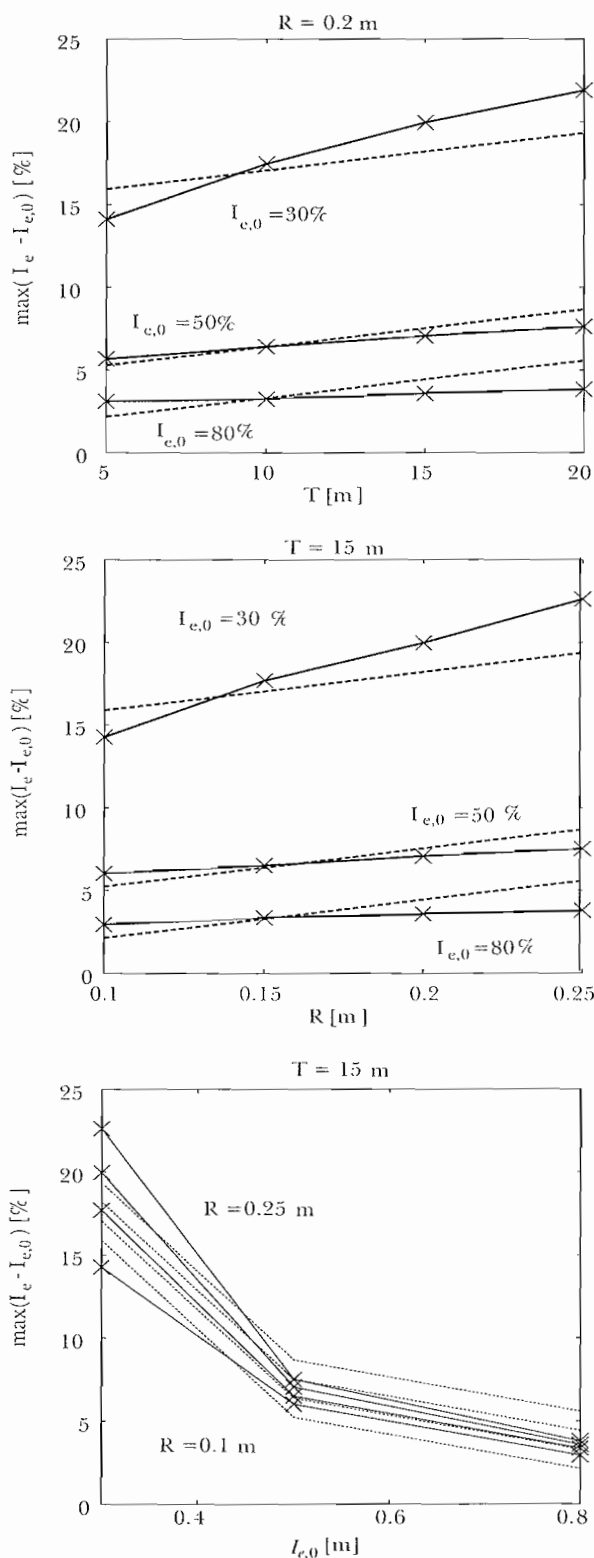


Fig. 6 – Maximum relative density minus initial relative density $I_{e,0}$ for well compactable soil (Schlabendorf sand) after pile driving. Continuous lines are results of finite element analysis; dash-dotted lines are results of Eq. 2. R is the pile radius, T is the depth.

Fig. 6 – Differenza tra densità relativa finale massima ed iniziale $\max(I_e)$, per un terreno ben compattabile (sabbia di Schlabendorf). Le linee continue sono i risultati delle analisi ad elementi finiti; le linee tratteggiate sono i risultati dell'Equazione 2. R è il raggio del palo e T è la profondità.

$$\frac{r(\max I_e)}{R} \approx c_0 + c_1 \frac{T}{T_0} + c_2 I_{e,0} \quad (3)$$

with

compactability	c_0	c_1	c_2
well	-1.56	-0.18	11.2
medium	1.91	-0.50	8.92
poorly	3.65	-0.68	9.46

2.3 Range of compaction

The range of compaction is in all cases:

$$\frac{r_V}{R} \approx 20 \quad (4)$$

2.4 Area of loosening

For medium or poorly compactable soils, and for well compactable soils with $I_{e,0} > 0.5$ the range of reduced density can be estimated as

$$\frac{r_A}{R} \approx d_0 + d_1 \frac{R}{r_0} + d_2 \frac{T}{T_0} + d_3 I_{e,0} + d_4 I_{e,0}^2 \quad (5)$$

with

compactability	d_0	d_1	d_2	d_3	d_4
well	2.94	-0.0085	-0.13	-8.33	11.4
medium	1.32	-0.0022	-0.17	-1.01	5.05
poorly	-0.33	0	0	5.48	1.17

3. Example

To illustrate the use of the equations the calculation of the relative density after pile driving in well, medium and poorly compactable soils is presented. The initial relative density is $I_{e,0} = 0.3$, the pile radius is $R = 0.25$ m. The density distribution is calculated in $T = 5$ m depth. The pile tip is deeper than 10 m.

Relative density at pile surface: First the change of the relative density at the pile surface can be calculated with (1). This results for well compactable soil

$$I_e(R) - I_{e,0} \approx 0.3 + 0.00411 \frac{R}{r_0} + 0.025 \frac{T}{T_0} - 0.89 I_{e,0}$$

with the limit radius $r_0 = 0.01$ m and the limit depth $T_0 = 5$ m

$$I_e(R) - I_{e,0} \approx 0.3 + 0.00411 \frac{0.25}{0.01} + 0.025 \frac{5}{5} - 0.89 \cdot 0.3 = 0.16$$

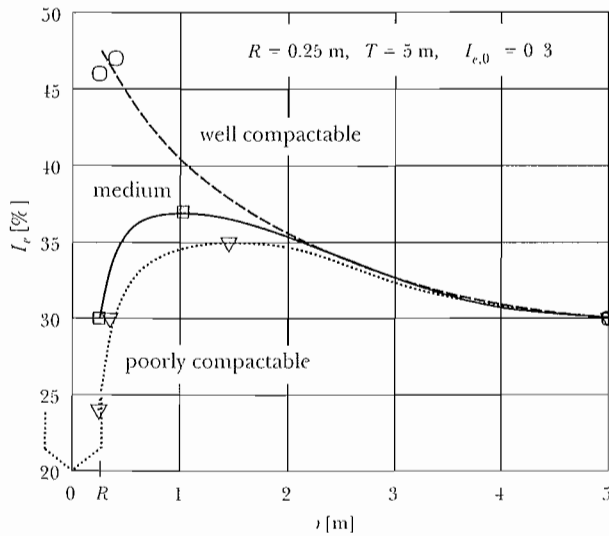


Fig. 7 - Approximated relative densities after pile driving.
 Fig. 7 - Densità relative approximate dopo l'infissione del palo.

The relative density after pile driving at the pile surface is $I_e(R) \approx I_{e,0} + 0.16 = 0.46$.

For medium and poorly compactable soils the relative densities calculated with (1) are $I_e(R) \approx 0.30$ and $I_e(R) \approx 0.24$, respectively.

Maximum relative density: The maximum relative density and its distance to the pile center can be calculated with (2) and (3).

This is for well compactable soil

$$\max(I_e - I_{e,0}) \approx 0.391 + 0.0023 \frac{R}{r_0} + 0.011 \frac{T}{T_0} - 1.22 I_{e,0} + 0.8591 I_{e,0}^2 = 0.17$$

and

$$\frac{r(\max I_e)}{R} \approx -1.56 - 0.18 \frac{T}{T_0} + 11.2 I_{e,0} = 1.6$$

The maximum relative density is then $\max(I_e) \approx I_{e,0} + 0.17 = 0.47$ in $r \approx 1.1R = 0.4$ m distance of the pile center.

For medium compactable soils is $\max(I_e) \approx 0.37$ in $r \approx 1.0$ m, and for poorly compactable soils is $\max(I_e) \approx 0.35$ in $r \approx 1.5$ m.

Range of compaction: The range of compaction is for all three soils with (4)

$$r_V \approx 20R = 5 \text{ m}$$

Area of loosening: In this example only for poorly compactable soils the density at the pile surface

is smaller than the initial density. The area of loosening can be estimated with (5)

$$\frac{r_A}{R} \approx -0.33 + 5.48 I_{e,0} + 1.17 I_{e,0}^2 = 1.4$$

compactability	$I_e(R)$	$\max I_e$	r m	r_V m	r_A m
well	0.46	0.47	0.4	5	-
medium	0.30	0.37	1.0	5	-
poorly	0.24	0.35	1.5	5	1.4

The radius of the loosened area is $r_a \approx 1.4R = 0.4$ m.

Density distribution: The characteristic points are collected in the following table - the relative density at the pile surface $I_e(R)$, the maximum relative density $\max I_e$ at the distance r from the pile center, the range of the compaction r_V and the radius of the loosened area r_A :

This characteristic points are plotted in Fig. 7. The density distribution in between this points can then be estimated as smooth curves.

Notes

⁽¹⁾ SALGADO *et al.* [1997, p. 346] state: Cavity expansion from zero initial radius to any finite radius is mathematically equivalent to expansion of an existing cavity all the way to infinity.

References

ABAQUS (1998) - *Version 5.8*. Hibbit, Karlson & Sorenson Inc., Rhode Island, U.S.A.
 CUDMANI R. (2000) - *Mechanismen bei der statischen, alternierenden und dynamischen Penetration in nichtbindigen Böden*. Heft 151, Institut für Bodenmechanik und Felsmechanik, Universität Karlsruhe.
 DAVIDSON J., MORTENSEN R.A., BARREIRO D. (1981) - *Deformations in Sand around a Cone Penetrometer Tip*. Soil Mechanics and Foundation Engineering, Tenth International Conference, vol. II, pp. 467-470.
 HERLE I. (2000) - *Hypoplastizität und Granulometrie einfacher Korngerüste*. Heft 151, Institut für Bodenmechanik und Felsmechanik, Universität Karlsruhe.
 Hochenwarter G. (2000) - *Verdichtungswirkung von Rammpfählen*. Diplomarbeit, Institut für Geotechnik und Tunnelbau, Universität Innsbruck.
 RODDEMAN D. (1997) - *A hypoplasticity routine for ABAQUS*. European Union Projekt "FEM-Imple-

mentation of Hypoplasticity”, Projekt n. ER-BCHBGCT 940554; <http://geotechnik.uibk.ac.at/res/FEhypo.html>.

SALDAGO R., MITCHELL J.K., JAMIOLKOWSKI (1997) – *Cavity Expansion and Penetration Resistance in Sand*. Journal of geotechnical and geoenvironmental engineering, pp. 344-354.

VON WOLFFERSDORFF P.-A. (1996) – *A hypoplastic relation for granular materials with a predefined limit state surface*. Mechanics of Cohesive-Frictional Materials, pp. 251-271.

Sommario

Durante l'infissione di un palo, il terreno è spostato radialmente. Ci si può quindi attendere che il terreno attorno ad esso risulti compattato. Un ampio numero di studi numerici con diversi modelli per terreni senza coesione, differenti diametri del palo e densità iniziali hanno mostrato che si verifica in effetti tale compattazione. Tuttavia, specialmente per terreni addensati o poco compattabili, c'è anche una zona di terreno attorno al palo in cui il terreno diventa più sciolto. Scopo dell'articolo è quello di fornire una stima approssimata della densità relativa attorno ad un palo infisso.